Applied Energy 186 (2017) 457–469

Contents lists available at ScienceDirect

Applied Energy

journal homepage: www.elsevier.com/locate/apenergy

# An experimental and theoretical investigation of the extent of bypass air within data centres employing aisle containment, and its impact on power consumption

Morgan Tatchell-Evans [a], Nik Kapur [a], Jonathan Summers [a,*], Harvey Thompson [a], Dan Oldham [b]

[a] School of Mechanical Engineering, University of Leeds, Leeds LS2 9JT, United Kingdom
[b] Digiplex London 1 Ltd, Highbridge, Oxford Road, Uxbridge UB8 1HR, United Kingdom

## HIGHLIGHTS

- Experimental investigation of bypass of cooling in data centres employing aisle containment systems.
- Effect of bypass on total power consumption investigated using a new system model.
- Practical measures for reducing bypass shown to reduce power consumption.
- Optimum level of aisle pressure investigated.

## ARTICLE INFO

*Article history:*
Received 14 December 2015
Received in revised form 9 March 2016
Accepted 17 March 2016
Available online 5 April 2016

*Keywords:*
Data centre
Thermal management
Bypass air
Aisle containment
Energy efficiency
System model

## ABSTRACT

A combination of laboratory experiments and a system model are used to carry out the first investigation into the potential for cold air to bypass IT equipment within data centres (DCs) employing aisle containment, and the effect of this bypass on DC electricity consumption. The laboratory experiments involved applying a differential pressure across commercially available server racks and aisle containment systems and measuring the resulting air flow. The potential to minimise bypass by sealing leakage paths and redesigning racks was investigated and quantified experimentally. A new system model is developed using a combination of manufacturer data, empirical relationships and experimental results to predict the impact of bypass on the power consumption of the various components of a DC's cooling infrastructure. The results show that, at typical cold aisle pressures, as much as 20% of the supplied air may bypass servers by finding alternate paths through the server rack itself. This increases the required flow rate from air conditioning units (ACUs). The system model predicts that: (i) practical measures undertaken to reduce this bypass could reduce total power consumption by up to 8.8% and (ii) excessive pressure differentials across the containment system could also increase power consumption, by up to 16%.
© 2016 The Authors. Published by Elsevier Ltd. This is an open access article under the CC BY license (http://creativecommons.org/licenses/by/4.0/).

## 1. Introduction

Energy use in residential and commercial buildings reportedly accounted for over 24% of total global energy consumption in 2012 [1], with this figure ranging from 20% to 40% in individual, developed countries [2]. Energy consumption in buildings has recently been predicted to rise by 31% between 2012 and 2040 [1]. Accordingly, it has been a focus of political initiatives to limit energy consumption for the past four decades, and has received much attention from the research community [3,4]. Heating, ventilation and air conditioning accounts for around half of energy consumption in buildings [2], and air conditioning specifically is expected to contribute significantly to the expected growth to 2040 [1,2]. Efforts within the research community to improve the efficiency of air conditioning systems have focused primarily on improving the coefficient of performance (COP) of the cooling system under a given set of air supply and return temperatures and flow rates, with savings achievable through changes to the management of air flows having received relatively little attention [5]. However, investigations into the benefits of reducing the mixing of hot and cold air streams through intelligent positioning of supply and return vents have shown this approach to have great potential for reducing energy consumption. Specifically, investigations focusing on air conditioning for thermal comfort, industrial food refrigeration and cooling of manufacturing facilities have

* Corresponding author.
*E-mail address:* J.L.Summers@leeds.ac.uk (J. Summers).

http://dx.doi.org/10.1016/j.apenergy.2016.03.076
0306-2619/© 2016 The Authors. Published by Elsevier Ltd.
This is an open access article under the CC BY license (http://creativecommons.org/licenses/by/4.0/).

**Nomenclature**

*Greek symbols*

| | |
|---|---|
| $\mu$ | dynamic viscosity (Pa s) |
| $\eta$ | efficiency (no units) |
| $\rho$ | density (kg m$^{-3}$) |

*Symbols*

| | |
|---|---|
| $a$ | width of channel (m) |
| $b$ | height of channel (m) |
| $c_p$ | specific heat capacity (J kg$^{-1}$ K$^{-1}$) |
| $D_h$ | hydraulic diameter (m) |
| $E$ | power consumption (kW h) |
| $f$ | friction factor (no units) |
| $k$ | loss coefficient (no units) |
| $L$ | length (m) |
| $\dot{m}$ | mass flow rate (kg s$^{-1}$) |
| $p$ | pressure (Pa) |
| $\dot{Q}$ | heat load/generation (W) |
| $Re$ | Reynolds number (no units) |
| $u$ | average velocity (m s$^{-1}$) |
| $\dot{V}$ | volumetric flow rate (m$^3$ s$^{-1}$) |

*Acronyms*

| | |
|---|---|
| ACU | air conditioning unit |
| CFD | computational fluid dynamics |
| COP | coefficient of performance |
| CW | chilled water |
| DC | data centre |
| HACA | hot aisle/cold aisle |
| LMTD | logarithmic mean temperature difference |
| PA | process air |

*Subscripts*

| | |
|---|---|
| ½ | up/downstream |
| BP | bypass |
| CA | cold aisle |
| CH | between hot and cold aisle |
| *con* | contraction |
| *eco* | economiser |
| *exp* | expansion |
| HA | hot aisle |
| *i*/*o* | at entrance/exit |
| *l* | laminar |
| PA | process air |
| *req* | required |
| *slot* | slot |
| *t* | turbulent |
| *T* | relating to the whole data centre facility |

predicted potential energy savings of 9–50% [6–9], 47% [10] and 63% [11], respectively, using this approach. The savings are accrued through reductions in the required conditioned air flow rate (which leads to savings in fan power) [6,7], and the potential to increase the supply air temperature, which increases the COP of chillers [6,7] and reduces their required operating hours (where free cooling is available) [7].

Data centres (DCs) are buildings which facilitate the operation of large quantities of computing equipment, and form the backbone of today's digital infrastructure [12]. They are energy-intensive facilities, with typical power densities of 540–2200 W/m$^2$, and extreme cases exceeding 10 kW/m$^2$ [13]. The DC industry has recently been estimated to account for 1.4% of global electricity consumption [14]. The compound annual growth rate (CAGR) of this electricity consumption from 2007 to 2012 has been estimated as 4.4% [14], much higher than the 2.1% projected for total global electricity demand from 2012 to 2040 [1]. Unchecked, this growth could have serious implications for efforts to reduce carbon emissions over the coming decades [15,16]. Governments have begun to take action to drive efficiency improvements in DCs, with the aim of reducing costs and environmental impact [17–19]. Energy consumption in the sector has also attracted the attention of the research community, as will be detailed in the remainder of this section.

Air conditioning is required in DCs in order to remove the heat generated by the servers, preventing them from overheating, and typically accounts for 20–50% of a DC's total electricity consumption, $E_T$ [20]. Accordingly, the efficiency of cooling is a major focus of efforts to reduce DC electricity consumption, with good practice regarding air management, cooling equipment operating conditions and selection of efficient equipment forming the basis of academic and governmental studies and best practice guidelines [21,22]. This paper focuses on air management, since recent studies have highlighted the potential for energy savings through improvements in this area [23–33]. As with air conditioning for thermal comfort, efforts to minimise DC air conditioning energy consumption must be balanced against the need to maintain the desired thermal conditions. Poor air management can both increase energy consumption and compromise the thermal environment. Specifically, the potential for supplied cold air to bypass IT equipment, returning to the ACU without carrying out any useful cooling duties, is known to impair the efficiency of a DC's cooling system [26,34–36]. This "bypass" increases the rate at which cold air must be supplied in order to ensure that sufficient air is available to cool the servers. Efforts to minimise bypass must be balanced against the need to avoid 'recirculation', i.e. the transport of hot air from server outlets back into server inlets. This can cause servers to fail due to over-heating [37], leading to DC managers reducing the supply temperature of conditioned air, which reduces the COP of the cooling system [38]. The goal is thus to distribute the cold air in such a way as to minimise the supply flow rate of cold air which is required in order to achieve an acceptably small level of recirculation, keeping server inlet temperatures within AHRAE's recommended limits [39]. Improvements in air management have been highlighted both as a cause of recent improvements in DC cooling efficiency and as an area in which further efficiency improvements can be made [40].

In an effort to minimise both bypass and recirculation, most modern, purpose-built DCs are arranged in hot aisle/cold aisle (HACA) formation. Servers are housed in rows of racks, with racks in adjacent rows aligned in opposite orientations, such that server inlets face each other into aisles into which cold air is supplied (termed cold aisles). The servers contain fans which draw the cold air over the heat generating components. Server outlets then face each other in hot aisles, from which hot air returns to the ACUs [37]. Segregation of hot and cold air streams is increasingly being further enhanced through the introduction of solid barriers separating hot and cold aisles, commonly referred to as aisle containment systems [34,35,40]. Fig. 1 shows diagrammatical representations of DCs employing HACA formation and cold aisle

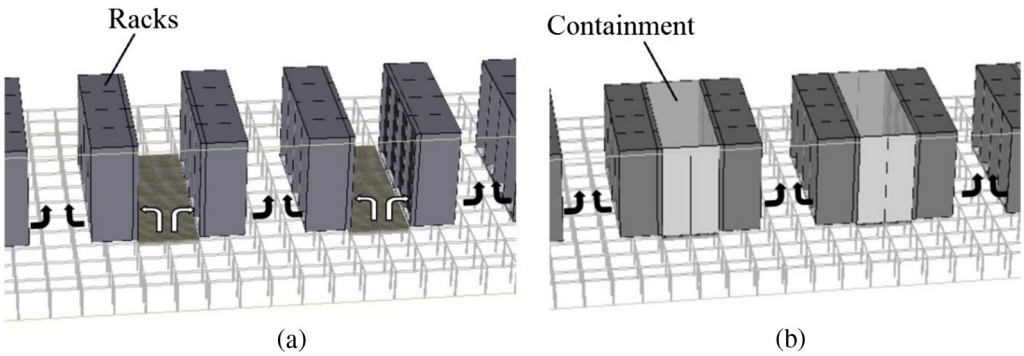


**Fig. 1.** (a) Diagram of DC in HACA formation and (b) diagram of cold aisle containment system. Paths of cold and hot air are shown in white and black arrows, respectively.

containment, with the air supplied from an underfloor plenum. Some bypass still occurs in contained systems, since over supply of cold air is required to minimise recirculation [34,41]. This produces a pressurisation of the cold aisle, causing air to escape through the containment system, or through the racks themselves. White papers, equipment specifications and trade journals propose pressure differentials between the hot and cold aisles, $\Delta p_{CH}$, ranging from 2 to 20 Pa [42–46], although this has not been studied extensively from an academic perspective.

Numerous recent journal publications have investigated a range of methods for optimising the distribution of cold air in a DC not employing aisle containment, with the goal of minimising bypass and recirculation. Computational fluid dynamics (CFD) simulations and experimental work have been used to investigate the impact of ceiling height [23] and placement of obstructions within the underfloor plenum [24] on distribution of cold air, and the relative benefits of supplying cold air from above and below [25–28]. The potential for controlling the distribution of cold air by tuning the open areas of floor grilles through which air is supplied to the DC has also been investigated [29].

The effect of aisle containment on DC cooling has been investigated experimentally by Arghode et al. [34] and in CFD simulations by numerous authors [26,31,32,35,47]. It is not possible to determine the total level of bypass in the contained data centres studied in Arghode et al.'s work since only the flow rates through the racks and ACUs were measured [34]. This implies that the authors have neglected to account for the potential for air to pass through the racks whilst avoiding the server inlets. Arghode's results show that roughly 10% of the air supplied to the cold aisle bypassed the racks, at $\Delta P_{CH} = 6.2$ Pa, with no other levels of $\Delta P_{CH}$ having been investigated [46]. The only computational model to be reported which considers bypass through the server racks is from Alkharabsheh et al. [41]. Here, rack bypass is allowed through 5 cm wide channels down the sides of the equipment rails in each rack, and similarly through channels at various potential leakage points identified visually in the aisle containment structure. All of these channels are assigned the same percentage open area, which is selected via a calibration process in which simulation results are compared with experimental measurements. The effect of bypass on energy consumption is not discussed, with the focus of the analysis being the air temperatures within the cold aisle, which were shown to occupy a narrower range where containment was employed. A later paper from the same lead author used the same model to show that increasing the percentage open area reduced the flow rate through servers (at constant ACU flow rate) and increased recirculation, which implies that bypass also increased [30]. This paper also reported that 4.6–13.4% of cold air supplied to the cold aisle bypassed the servers, depending on the ACU fan speed. However, there was no discussion of $\Delta P_{CH}$ or of the relative importance of bypass through the racks and containment system. Other CFD simulations have been used to demonstrate the potential reductions in electricity consumption resulting from the implementation of aisle containment: Schmidt et al. [31] reported a reduction in $E_{ACU}$ of 59%, whilst Shrivastava et al. [32] found a 33% reduction in the electricity consumption of the cooling infrastructure. Schmidt et al. [31] and Shrivastava et al. [32] report bypass percentages within contained systems of 3.1 and 13% respectively, although neither disclose any information regarding the model detail governing bypass from the contained aisles, nor do they report the value of $\Delta p_{CH}$ [31,32]. For comparison, monitoring of server and ACU inlet and outlet temperatures carried out by Salim and Tozer [20] at 40 DCs not employing aisle containment found that, on average, 50% of cold air supplied by the ACUs bypassed the servers. It follows that the aforementioned investigations have shown the potential for aisle containment to reduce bypass and improve thermal conditions, although there is still a need for further investigation to determine the extent to which aisle containment can reduce electricity consumption, and how these systems can be optimised.

The impact of bypass on $E_T$ depends on the responses of the various electricity consuming components to the changing conditioned air flow rates and temperatures caused by bypass. Numerous models of HVAC systems in thermal comfort applications are available which predict the energy consumption of such systems under different conditions or arrangements. Nguyen et al. [48] produced an extensive review of these models, which are typically grouped into data-driven models (such as frequency domain models, statistical models and data mining algorithms), physics-based and grey box models. Data-driven models require the availability of substantial information regarding the performance of the system under different conditions. Physics-based models typically include conductive heat transfers through elements such as walls and windows, heat gains from the sun and electrical equipment, convective heat transfers, heat transfers at the heating and cooling coils, control systems for coolant and chilled water flow rates, fans and pumps, boilers, chillers, heat pumps and cooling towers. Grey box models use measured data pertaining to the system's true performance to inform the parameters used in the equations underpinning a physics-based model.

A number of system models have been developed for DCs, typically with the aim of enabling the facility power consumption associated with various configurations and conditions to be predicted [33,38,49–53]. In all cases, they fall into the category of physics-based models. The components of the models typically include servers, heat exchangers, ACUs, chillers, cooling towers and chilled water (CW) pumps. The various models use a combination of manufacturer specifications, thermodynamic analysis and empirical models to define the performance of the components. Various approaches have been used to model the heat transfers in heat exchangers in DC system models, including fundamental

analysis to determine the thermal resistances at the heat exchangers [50], heat transfer effectiveness-NTU methods [33] and empirical relationships [38]. Most of the models assume no bypass occurs. Of the 2 that do include bypass, one uses CFD simulations to predict levels of bypass and recirculation within a data centre not employing aisle containment [52], whilst the other defines bypass as a model parameter without justification of the values used [50]. The discussions around these models fail to examine the effect of bypass on energy consumption. Since the extent of bypass varies significantly between DCs, and has a large impact on energy consumption, bypass should be considered an important parameter in any DC model. Efforts within the industry in recent years to reduce bypass through measures such as the introduction of HACA formation and aisle containment provide further incentive to quantify the likely benefits of bypass reduction.

This review of the literature has demonstrated that there has been no prior experimental investigation reported in the peer reviewed literature which properly quantifies bypass within a DC employing aisle containment. Only one computational model has been presented which considers bypass through racks, with the associated papers [30,41] neglecting to (i) investigate the relationship between $p_{CH}$ and bypass, (ii) disclose the relative importance of bypass through racks and through the containment system and (iii) experimentally verify the approach to modelling of bypass. The experimental results presented in this paper represent the first quantification of bypass through racks in a contained aisle system, and the first investigation into the potential to minimise this bypass through careful rack design. A physics-based system model is developed which enables the first investigation within the peer reviewed literature into the effect of this bypass on $E_T$. The model is the first to consider the impact of $\Delta p_{CH}$ on (i) bypass, (ii) server flow rates and (iii) server fan power consumption. The paper also provides the first discussion within the peer-reviewed literature of the optimum value of $\Delta p_{CH}$ and the effect of bypass within racks on $E_T$.

## 2. Material and methods

### 2.1. Bypass through server racks

Server racks are fitted with equipment rails sized to accommodate IT equipment of standard 483 mm (19 in.) width. The rails contain 'slots' into which IT equipment may be installed. Racks usually contain some empty slots, which should be filled with blanking panels to prevent the slots from providing paths for bypass (or 'leakage paths'). Space exists on either side of the equipment rails, as well as above and below them, which may provide undesired, additional leakage paths. There may also be the potential for air to escape through the top, bottom or sides of the rack, after entering the rack front, but prior to passing into the server inlets. These leakage paths are shown in Fig. 2, illustrated by the arrows. Rack manufacturers use various techniques to minimise the potential for flow through these paths, filling the space with sheet metal, foam, rubber strips, and brushes.

Attempts to minimise bypass through cold aisle containment may also be compromised by empty slots within server racks, since in some DCs these are not routinely filled with blanking panels [40]. The volumetric flow rate, $\dot{V}_{slot}$, through such a slot, may be estimated by modelling the flow as being through a rectangular channel which is 430 mm wide, 44.5 mm deep and 724 mm long, which represents the space between 2 typical servers separated by an empty slot [54]. Such a flow is depicted in Fig. 3. The resistance offered by the entrance and exit to the slot may be estimated by recognising that these flow features represent flow from a reservoir into a pipe (a contraction) and from a pipe into a reservoir (an expansion), respectively. The pressure drop across these features can be calculated using Eqs. (1) and (2), respectively [55]. Here, $p_C$, $p_{con}$, $p_{exp}$ and $p_H$ are the gauge pressures in the cold aisle, immediately after the contraction, immediately before the expansion and in the hot aisle, respectively; $\rho$ is the density of the air; $u$ is the average air velocity within the slot; and $k_{con}$ and $k_{exp}$ are the loss coefficients relating to the contraction and expansion, respectively. $k_{con}$ and $k_{exp}$ may be approximated as 0.5 and 1, respectively, for this kind of contraction and expansion [55].

$$p_C - p_{con} = 0.5\rho k_{con} u^2 \text{ [55]} \quad (1)$$

$$p_{exp} - p_H = 0.5\rho k_{exp} u^2 \text{ [55]} \quad (2)$$

Losses within a rectangular channel are affected strongly by whether the flow regime is laminar or turbulent [56]. For laminar flow, the pressure drop along the length of the channel may be estimated using Eq. (3), where $f$ is the friction factor, $L$ is the length of the channel and $D_h$ is the hydraulic diameter. $D_h$ is given by Eq. (4), where $a$ and $b$ are the width and depth of the channel, respectively

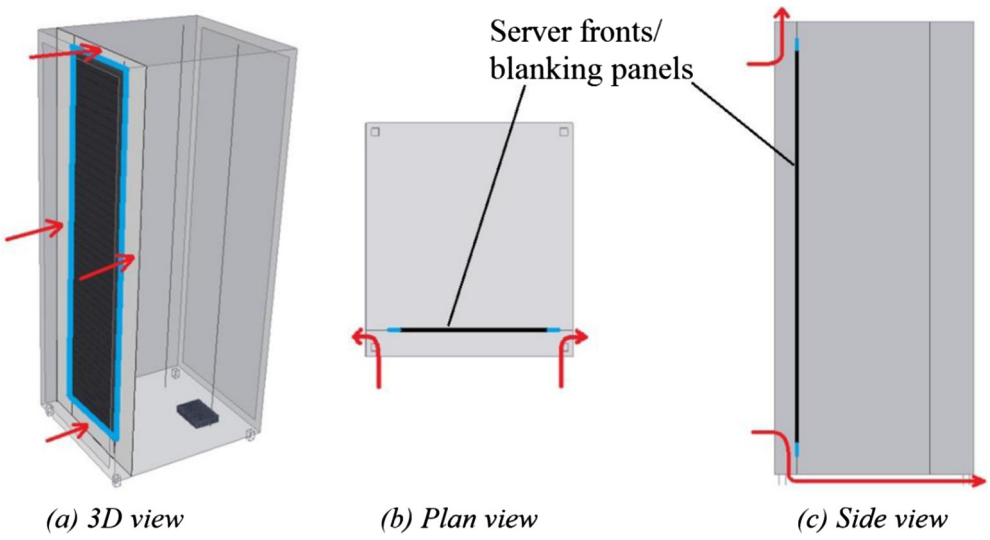


**Fig. 2.** Rack leakage paths (a) above, below and at sides of equipment rails (b) through sides of rack and (c) through top and bottom of rack. The black lines in (b) and (c) represent the plane coinciding with server fronts in occupied slots, and blanking panels in unoccupied slots.

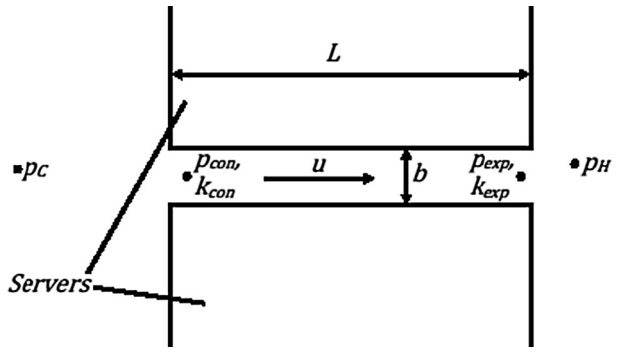


**Fig. 3.** Flow through an empty slot.

[56]. $f$ is dependent on the aspect ratio of the channel, $a/b$, and for a channel with $a = 0.0445$ m and $b = 0.437$ m is given by Eq. (5) [56]. $Re$, the Reynolds number, is given by Eq. (6), where $\mu$ is the dynamic viscosity. Combining Eqs. (3)–(6) gives Eq. (7), where $u_l$ is the average velocity within the slot in the laminar case.

$$p_{con} - p_{exp} = 0.5 f \rho L u^2 / D_h \quad [56] \tag{3}$$

$$D_h = 2ab/(a+b) \quad [56] \tag{4}$$

$$f = 84.4/Re \quad [56] \tag{5}$$

$$Re = \rho u D_h / \mu \quad [56] \tag{6}$$

$$p_{con} - p_{exp} = 10.55 \mu L u_l (a+b)^2 / a^2 b^2 \tag{7}$$

Laminar flow generally dominates in such channels where $Re < 2000$, with turbulence dominating where $Re > 4000$ [56]. An initial assumption of laminar flow allows us to combine Eqs. (1), (2) and (7), whilst noting that $\Delta p_{CH} = (p_C - p_{con}) + (p_{con} - p_{exp}) + (p_{exp} - p_H)$ and $u = u_l$, giving Eq. (8). Thus, $u_l$ may be determined for a given $\Delta p_{CH}$ using the quadratic formula (assuming that $\mu = 2.2 \times 10^{-5}$ Pa s and $\rho = 1.2$ kg m$^{-3}$ [58]).

$$0.5\rho(k_{con} + k_{exp})u_l^2 + \frac{10.55\mu L(a+b)^2}{a^2 b^2} u_l - \Delta p_{CH} = 0 \tag{8}$$

Having determined $u_l$, $Re$ can be found using Eq. (6). This allows the validity of the assumption of laminar flow to be determined. If $Re > 2000$, the calculation must be repeated using a different method. Jones [57] reviewed the results of tests carried out in rectangular channels of various aspect ratios, finding that Eq. (9) fitted the results well for turbulent flow. Here, $u_t$ is the average velocity within the slot for the turbulent case, $Re$ is again given by Eq. (6), but $D_h$ is given by Eq. (10). $f$ is again related to the pressure drop via Eq. (3) [57]. Combining Eqs. (1)–(3), noting that $u = u_t$ and re-arranging to make $u_t$ the subject gives Eq. (11). Combining Eqs. (6), (9) and (11) gives Eq. (12).

$$f^{-0.5} = 2\log_{10}(f^{0.5} Re) - 0.8 \quad [57] \tag{9}$$

$$D_h = 2\left[\frac{2}{3} + \frac{11}{24}\frac{a}{b}\left(2 - \frac{a}{b}\right)\right] ab/(a+b) \quad [57] \tag{10}$$

$$u_t = \left(\frac{2\Delta p_{CH}}{\rho\left(k_{con} + k_{exp} + \frac{fL}{D_h}\right)}\right)^{0.5} \tag{11}$$

$$f^{-0.5} - 2\log_{10}\left[\frac{f^{0.5}\rho D_h}{\mu}\left(\frac{2\Delta p_{CH}}{\rho\left(k_{con} + k_{exp} + \frac{fL}{D_h}\right)}\right)^{0.5}\right] + 0.8 = 0 \tag{12}$$

So for a given $\Delta p_{CH}$, $f$ may be calculated by applying the bi-section method to Eq. (12) (after calculating $D_h$ using Eq. (9)). $u_t$ may then be calculated using Eq. (11). Whether the flow is laminar or turbulent, $\dot{V}_{slot}$ may then be calculated according to $\dot{V}_{slot} = uab$, after setting $u$ equal to $u_l$ or $u_t$ as appropriate. For flow in the transition region, $u$ may be approximated using a linear interpolation between $u_l$ at $Re = 2000$ and $u_t$ at $Re = 4000$, taking $Re$ for the given $\Delta p_{CH}$ as the average of those predicted using the laminar and turbulent methods. For $2 < \Delta p_{CH} < 20$, it was found that $Re > 4000$, indicating turbulent flow,and that $\dot{V}_{slot}$ ranged from 25 to 83 l/s. The calculation process is illustrated in Fig. 4.

To put these figures in context, at typical rack power densities of 12 kW/rack [59] and temperature rise across the servers, $\Delta T$, of 12.5 K [38,60], the flow rate of air required to cool the servers may be calculated by applying conservation of energy, so that $E_{server} = \dot{m}_{server} c_p \Delta T$. Here, $E_{server}$ is the rack power consumption, $\dot{m}_{server}$ is the mass flow rate through the servers, $\Delta T$ is the temperature rise of the air across the servers and $c_p$ is the specific heat capacity of air, held constant at 1.005 kJ/kg K [58]. Since $\dot{m}_{server} = \dot{V}_{server}\rho$, (where $\dot{V}_{server}$ is the volumetric flow rate through the servers), $\dot{V}_{server}$ may be calculated, enabling the flow through a single empty slot within a rack to be quantified as representing 3.1–10.4% of the air passing through the rack over the same range of $\Delta p_{CH}$.

The value of $\Delta p_{CH}$ also affects flow rates through servers. Experiments reported by Brady [61] and in an industry white paper [62] have given an indication of the flow rates through idle and

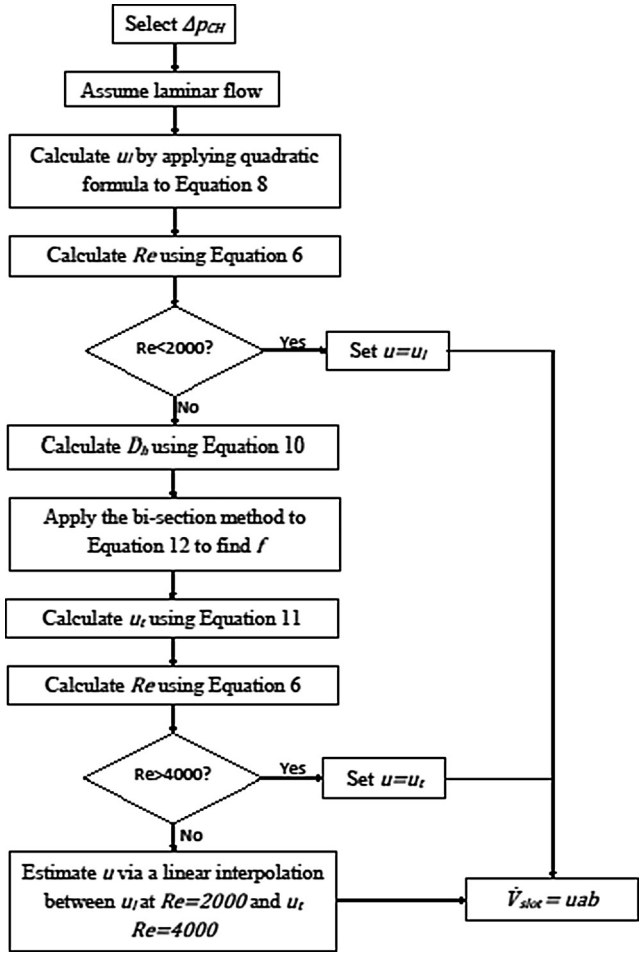


**Fig. 4.** Flow chart for $\dot{V}_{slot}$ calculation.

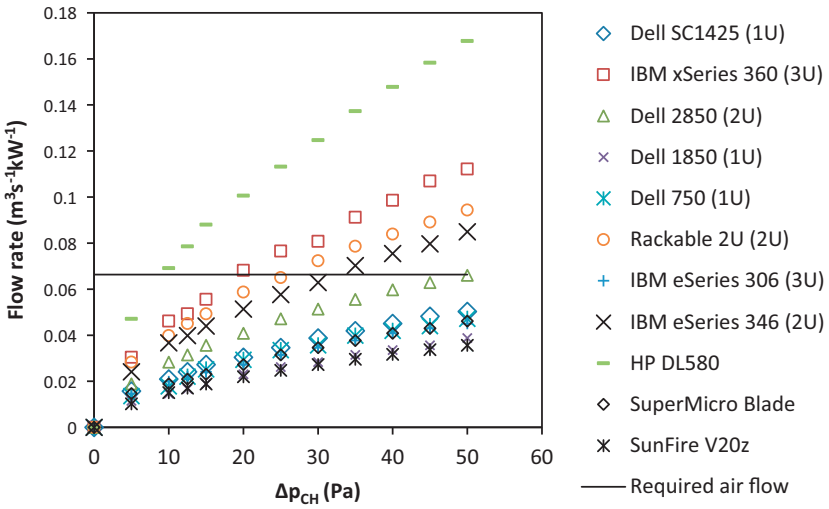


**Fig. 5.** Measured flow rates per kW of nameplate power consumption through switched off servers at a range of differential pressures, compared with air flow required for adequate cooling. Data from [62] except SunFire V20z from [61].

switched off servers subjected to external static pressures. The results for switched off servers are collected in Fig. 5, with the measured flow rates having been divided by the respective servers' nameplate power consumptions. No similar data has been published for active servers. Assuming $\rho = 1.2\ \mathrm{kg\ m^{-3}}$, $c_p = 1.005\ \mathrm{kJ\ kg^{-1}\ K^{-1}}$ and $\Delta T = 12.5\ \mathrm{K}$ [38,60], the flow rate required to cool a server as a function of server power consumption can be calculated as $1/(c_p \rho \Delta T) = 0.0663\ \mathrm{m^3\ kW^{-1}}$. This figure has been plotted as a horizontal line in Fig. 5, and shows that the majority of servers would require $\Delta p_{CH}$ to be greater than 30 Pa in order for sufficient air flow to occur without the action of server fans. This implies that typical values of $\Delta p_{CH}$ will not drive sufficient airflow through servers, and that server fans are required to ensure adequate cooling. Brady [61] also investigated the potential to cool servers using only a pressurised cold aisle, with server fans removed. The tests showed that under some conditions this resulted in overheating of servers. Server fan speeds are generally controlled to maintain appropriate central processing unit (CPU) temperatures [63]. Brady's test results demonstrate that whilst cold aisle pressurisation may be effective in cooling the server to some extent, server fans may still be needed to direct air to the hottest components if failures are to be avoided.

The extent to which $\Delta p_{CH}$ drives excess flow through servers also depends on the heat generated by the server ($Q_{server}$), since this affects the required air flow rate ($\dot{V}_{server}$). Server power consumptions are usually considerably lower than nameplate values due to low CPU utilisation, with many servers housed in DCs being obsolete, outdated or unused [64]. Utilisation rates vary between DCs, with cloud computing and high performance computing usually enabling higher utilisation [65–67]. Barroso et al. [68] reported data showing the CPU utilisation distribution against time from their measurements of more than 5000 servers in use in DCs, finding that they operated at a utilisation of between 10% and 50% for more than 70% of the sampling time. The same study stated that a typical energy efficient server used around 50% of its peak power consumption at 0% CPU utilisation, with this increasing linearly to 100% at full CPU utilisation.

The effect of bypass on $E_T$ must be influenced by the density of IT within the facility. Low IT densities correspond to low flow rates of air required for server cooling, increasing the significance of bypass air flow rates which are determined by $\Delta p_{CH}$ and the permeability of the racks and containment system. DCs often operate well below their design capacity since they are designed to cope with peak workloads which may occur infrequently [69,70] and to accommodate future expansion [71].

### 2.2. Experimental methods

An 800 mm wide commercial server rack was obtained. The rack was 42U high, meaning that it was designed to accommodate 42 pieces of IT equipment each with a standard height of 44.45 mm. Blanking panels were installed into the equipment slots, thus ensuring that any flow measured through the rack represented bypass which would occur within a contained system, excluding any bypass within the area occupied by the equipment slots. No IT equipment was installed.

A duct was constructed from corrugated plastic, to enclose the air flow driven through the rack. One end of the duct was attached to a fan, the other to the rack. A side view diagram and a photograph of the setup are shown in Fig. 6. Section A was 2 m long and of constant cross-section, allowing a uniform flow to develop. Section B had an expanding width, up to 800 mm. Section C had an expanding height, up to 2010 mm. Consequently, the end of Section C was large enough to accommodate the rack. The interfaces between the fan and duct, duct and rack and individual pieces of corrugated plastic were sealed using an appropriate adhesive tape.

A hole was inserted towards the end of Section A to enable flow measurement using a hot wire anemometer. The anemometer was positioned such that the sensor was at the centre of the section. For most of the measurements an Omega HHF2005HW [72] anemometer was used, which has a resolution of ±0.1 m/s. For the internal dimensions of the channel used, this corresponds to a resolution of ±2.4 l/s on volumetric flow rates. For speed measurements below 2.0 m/s, an Airflow 'TA-2 2' anemometer was used [73]. This has a resolution of ±0.1 m/s for speeds above 0.5 m/s and ±0.05 m/s below 0.5 m/s. The latter corresponds to a resolution of ±1.2 l/s on the flow rates calculated. The volumetric flow rate through the duct was calculated as the product of the velocity and the cross-sectional area, with the velocity assumed to be constant across the section.

A second hole was inserted in Section C, as shown in Fig. 6. A length of tubing was inserted into this hole, with its other end attached to a manometer, which allowed the differential pressure between front and back of the rack, $\Delta p_{CH}$, to be measured. A Digitron 2080p manometer [74] was used for most of the pressure measurements, which has a resolution of ±0.1 Pa. For the first test

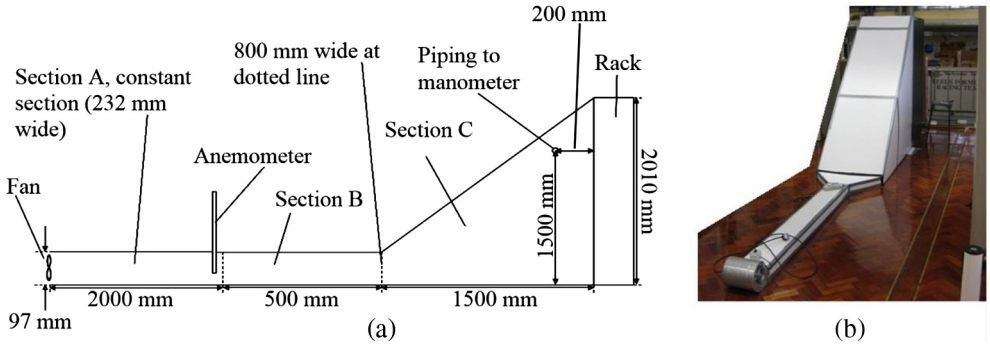


**Fig. 6.** (a) Schematic and (b) photograph of experimental set-up.

(denoted 'Single Rack Test 1' in Fig. 10), a KIMO HP 15 manometer was used, which has a resolution of ±1 Pa [75].

The key leakage paths were identified through observation and use of the anemometer. A series of experiments was performed, with measurements being taken after sealing each identified leakage path. For each configuration, anemometer and manometer readings were taken over a range of fan speeds. The fan was first set to the desired speed, and the manometer reading recorded after it had reached a constant value. An anemometer reading was then taken. The speed measurements were converted to volumetric flow rates by multiplying them by the cross sectional area of Section A of the duct.

Similar tests were carried out in a test DC, an enclosure measuring 4.0 × 3.4 m in footprint, and 3.5 m in height, which houses a row of 4 server racks (schematic shown in Fig. 7). Air was supplied into the cold aisle and allowed to exit from the hot aisle, with a partition installed above the racks to separate the hot and cold aisles. The interfaces between adjacent racks and between the racks and enclosure walls were sealed using a silicone sealant to prevent air flow in these regions. The flow rate through the supply duct was measured in the same way as for the single rack tests, using the Omega HHF2005HW anemometer [72]. Since the supply duct had a cross sectional area of 0.0731 $m^2$, this manometer's resolution of ±0.1 m/s corresponds to a resolution of ±7.31 l/s on flow rate measurements. A total of 9 speed measurements were taken across the cross-section of the duct, to account for variations of speed within the duct. These measurements were converted to a volumetric flow rate by integrating between the measurement points, assuming linear variation of speed and zero velocity at the wall of the duct. A differential pressure reading ($\Delta p_{CH}$) was taken between the cold aisle and the exterior of the test DC, using the Digitron 2080p manometer [74]. A commercially available aisle containment system was used, and the racks were fitted with blanking panels as with the single rack tests. The rack design was modified following the single rack tests, in an attempt to achieve a readily repeatable, well-sealed rack design. All modifications used standard parts available from the rack manufacturer.

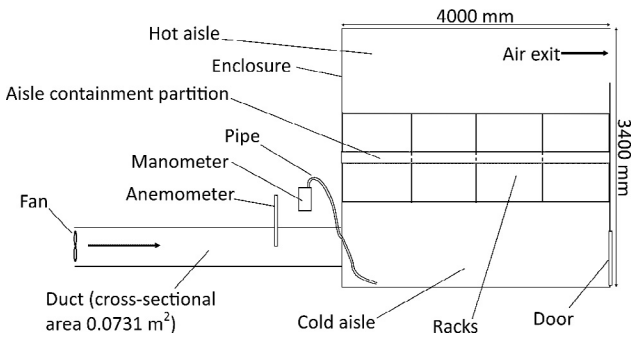


**Fig. 7.** Schematic of test DC (plan view, height of test DC is 3.5 m).

Initial measurements taken in the test DC found some leakage of air from the test DC to the surroundings. This was quantified and has been accounted for in the results presented in Section 3.1.

### 2.3. Description of the new system model

Fig. 8 shows a schematic of the physics-based system model constructed to predict the impact of bypass and cold aisle pressurisation on $E_T$, within a DC employing aisle containment. The model was run with an ambient temperature ($T_{amb}$) of either 11 °C (the average $T_{amb}$ for London [76]) or 30 °C. In the former case the CW loop used to cool the process air (PA) rejects heat to the ambient air, in an economiser consisting of a heat exchanger and fan. At $T_{amb}$ = 30 °C the CW is cooled mechanically in a chiller whose working fluid is cooled using ambient air. PA is supplied to the cold aisle at 25 °C, which is at the higher end of the range recommended by ASHRAE (18–27 °C) [77].

The bypass flow rate ($\dot{V}_{BP}$) is based on the results of the experiments described in Section 2.2, which are shown in Fig. 10. The flow rate is calculated by carrying out a linear interpolation between the flow rates measured at the pressure differential just below and just above that selected in the model. Where the pressure selected in the model is less than the lowest pressure at which a measurement was taken, the interpolation takes place between the origin and the lowest pressure measurement. The volumetric flow rate of air required through the server, $\dot{V}_{server}$, in order to absorb the heat generated by the server ($\dot{Q}_{server}$), is calculated using Eq. (13), assuming a temperature rise across the server, $\Delta T$, of 12.5 K [38,60]. The specific heat capacity, $c_p$, and air density, $\rho$, are held constant at 1.005 kJ/kg K and 1.2 kg/m³, respectively. The static pressure required to act across the server in order to achieve this flow, $\Delta p_{req}$, and the flow rate forced through the server as a result of the cold aisle pressure, are then identified from a server system curve determined experimentally by Brady [61]. This curve is for a SunFire V20z server, and agrees well with the equation $\Delta p_{server} = 38289\dot{V}^2_{server}$, where $\Delta p_{server}$ is the static pressure across the server.

$$\dot{Q}_{server} = \dot{V}_{server}\rho c_p \Delta T \tag{13}$$

Two options are considered for server fan speed control. With Option 1, the server fan speed is controlled so as to produce a pressure drop which, when added to $\Delta p_{CH}$, will produce $\Delta p_{req}$. With Option 2, the server fan speed is affected only by the server heat load, effectively assuming that the forced air flow does not take the path required for it to cool the CPU. The server fan speed in this case is controlled so as to produce $\Delta p_{req}$, with $\Delta p_{CH}$ being ignored. In each case, $\Delta p_{req}$ is determined from Brady's experimental results,

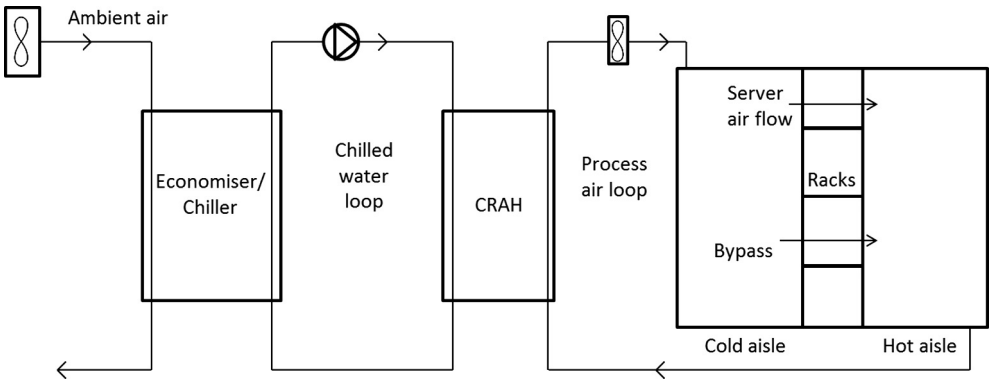


**Fig. 8.** Schematic of the system model including provision for bypass and aisle pressurisation.

collected from tests with fans from a SunFire V20z server [61]. Brady's data shows the relationship between flow rate and pressure drop generated by the fans at a range of power consumptions.

The power consumption attributed to servers within the model is based on the data reported by Barroso et al. [68], discussed in Section 2.1. The servers are divided into 10 blocks, each comprising 10% of the total number of servers. The power consumption of servers within each block as a percentage of maximum power consumption is shown in Fig. 9, with the distribution being set to match the findings of Barroso et al. Each rack is populated with sufficient servers that the total power consumption within the rack would be 12 kW, were each server to operate at its full capacity (representing a typical design rack power density [59]). Where Option 1 is selected for server fan speed control, the server power consumptions assigned under the Barroso distribution are reduced to account for the reduction in server fan power from that which would be required if no external static pressure acted across the server.

The power consumptions of the CW pump and the ACU and economiser fans ($E_{CW}$, $E_{ACU}$ and $E_{eco}$, respectively), are assumed to scale with the cube of their respective flow rates [38], such that $E = E_{ref}(\dot{V}/\dot{V}_{ref})^3$, where $E$ is power consumption, $\dot{V}$ is volumetric flow rate, and the subscript *ref* denotes the reference conditions. The reference conditions are taken from manufacturer specifications. For the ACU and economiser fans, $E_{ref}$ and $\dot{V}_{ref}$ are taken directly from Schneider Electric's Uniflair TD/UCV 0700 ACU [78]. This is an ACU designed for use in DCs. For the CW pump, a reference pressure drop, $\Delta p_{CW}$ and flow rate, $\dot{V}_{CW}$, are again taken from the Uniflair TD/UCV 0700. The same pressure drop is assumed to act in the heat exchanger at the economiser/chiller, with the two

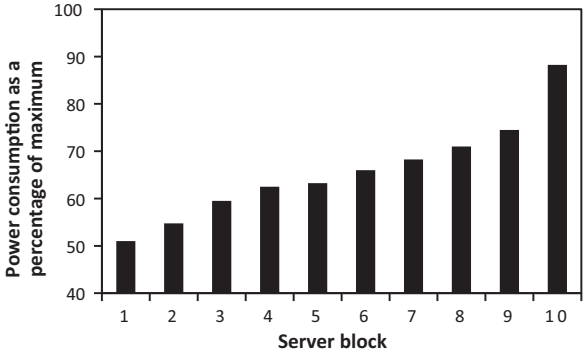


**Fig. 9.** Distribution of server power consumptions, with each block accounting for 10% of the total number of servers. Data from [68].

being summed to give the total pressure drop for the CW loop. The efficiency of the CW pump, $\eta_{CW}$, is taken to be 0.9, as is reported to be typical for such pumps by Salim and Tozer [20]. The reference power consumption is then calculated as $E_{ref} = 2\eta_{CW}\Delta p_{CW}\dot{V}_{CW}$. The heat generated by fans and pumps, $\dot{Q}_{fan/pump}$, is then calculated according to Eq. (14). The efficiency, $\eta$, is in both cases taken to be 0.9, which is again consistent with efficiencies reported by Salim and Tozer [20].

$$\dot{Q}_{fan/pump} = E_{fan/pump}\ (1-\eta) \tag{14}$$

A heat transfer rate, $\dot{Q}_{ref}$, and associated air and water flow rates, $\dot{V}_{water,ref}$, and $\dot{V}_{air,ref}$, and temperatures, are obtained from manufacturer data relating to the Uniflair TD/UCV 0700 ACU [78]. This allows a reference heat transfer coefficient, $h_{ref}$, to be calculated, using Eqs. (15) and (16) [79]. In Eq. (15), LMTD refers to the logarithmic mean temperature difference across the heat exchanger. In Eq. (16), the temperatures, $T$, are identified by the subscripts *air* and CW for air and chilled water, respectively, and $i$ and $o$, for the temperature at entrance to and exit from the heat exchanger, respectively.

$$h_{ref} = \dot{Q}_{ref}/(\mathrm{LMTD}) \tag{15}$$

$$\mathrm{LMTD} = \frac{(T_{air,i} - T_{CW,i}) - (T_{air,o} - T_{CW,o})}{\ln\left[\frac{T_{air,i}-T_{CW,i}}{T_{air,o}-T_{CW,o}}\right]} \tag{16}$$

Heat transfers in the ACU and economiser are modelled using Eq. (17). This is derived from experimentally verified relationships whose accuracy has been confirmed by numerous authors for gas to liquid fin and tube heat exchangers (commonly used in CW ACUs). For the gas side flow rate, $n$ varies from 0.581 to 0.681, depending on the heat exchanger design [80,81] (0.631 was used as the default value). For heat transfers from liquids flowing in a pipe, $h$ has been shown to be proportional to the liquid flow rate raised to the power 0.8 [82]. This can be applied to the liquid side of gas to liquid fin and tube heat exchangers. $\dot{V}_{water,ref}$ and $\dot{V}_{air,ref}$ are obtained from manufacturer data relating to the Uniflair TD/UCV 0700 ACU [78].

$$h = h_{ref}\left(\dot{V}_{water}/\dot{V}_{water,ref}\right)^{0.8}\left(\dot{V}_{air}/\dot{V}_{air,ref}\right)^{n} \tag{17}$$

The heat load on the ACU ($\dot{Q}_{ACU}$) is calculated using Eq. (18). Here, $E_{server\ fans}$ and $\dot{Q}_{server\ fans}$ are the power consumption and heat generation of the server fans, and $E_{servers}$ is the power consumption of the servers. $\dot{Q}_{server\ fans}$ is calculated by subtracting the air flow kinetic energy generated by the server fans from $E_{server\ fans}$. The air flow kinetic energy is given by the product of the pressure

and flow rate developed by the fans at $E_{server\ fans}$. The heat load on the economiser or chiller, $\dot{Q}_{eco/chiller}$, is the sum of $\dot{Q}_{ACU}$ and the heat generated by the ACU fans and CW pumps. Assuming efficiencies of 0.9, these heat loads may be calculated as $(1-0.9)E_{fan/pump}$.

$$\dot{Q}_{ACU} = E_{servers} - E_{server\ fans} + \dot{Q}_{server\ fans} \quad (18)$$

The CW flow rate is controlled so as to minimise $E_T$, which is calculated according to $E_T = E_{servers} + E_{ACU} + E_{CW} + E_{eco}$.

Where the chiller is in use, manufacturer data for Airedale's DeltaChill unit is used to inform the power input (for the compressor and fans) required to achieve the required cooling, which varies with $T_{amb}$ and the difference between the CW supply temperature and $T_{amb}$ [83]. This chiller is designed for use in DCs, and has a refrigerant loop designed to be cooled using ambient air. The manufacturer data shows how the input power and heat transfer rate vary with CW supply temperature, at a range of $T_{amb}$. The relationship at each $T_{amb}$ may be seen to approximate a straight line. A least squares fit was used to define the relationship at $T_{amb}$ = 30 °C, allowing the power consumption of the chiller under the given conditions to be calculated. Again, the CW flow rate is controlled so as to minimise $E_T$, which is calculated according to $E_T = E_{servers} + E_{ACU} + E_{CW} + E_{chiller}$.

## 3. Results

### 3.1. Bypass experiments

Fig. 10 shows the bypass percentages represented by the flow rates measured in the single rack and test DC experiments. The bypass percentages are calculated based on the flow rate that would be required to cool the servers contained in a rack operating at a typical IT power load of 12 kW [59] and $\Delta T$ of 12.5 K [38,60]. This is calculated by applying conservation of energy, i.e. $E_{server} = \dot{m}_{server} c_p \Delta T$. The effect of cold aisle pressurisation on server flow rates and server fan power consumption is ignored in this calculation. The 'Single rack' results are from tests carried out on commercially available racks. Test 1 used a rack which had been setup as recommended by the manufacturer, with Test 2 showing the results after the most prominent leakage paths had been sealed. This involved simply placing one strip of foam above the uppermost blanking panel, and one below the bottom panel. In order to achieve the percentage bypasses reported for Test 3, considerable effort was made in order to seal the many leakage paths identified, using adhesive tapes and foam strips. The results from the test DC used a modified, commercially available rack whose setup had been informed by the findings of the single rack tests, using standard parts, readily available from the rack manufacturer, to minimise bypass. Error bars are included in the graph, with the process used to calculate their magnitude being described in Section 4.1.

### 3.2. System model results

Figs. 11 and 12 show the results from the system model, with the effect of $\Delta p_{CH}$ and implementation of bypass minimisation measures on $E_T$ being investigated in each case. The results denoted as high bypass correspond to the bypass figures shown in Fig. 10 for 'Single rack Test 1'. The results denoted as low bypass correspond to bypass figures from the test DC. Fig. 11 additionally investigates the impact of the algorithm used to determine the server fan power consumption. Here, the normalised power consumption at $\Delta p_{CH}$ = 5 Pa with high bypass is set at unity for server fan option 2, with all other power consumptions shown as a proportion of this figure. The results are shown with $T_{amb}$ = 11 °C (i.e. with no mechanical cooling) and $T_{amb}$ = 30 °C (i.e. with mechanical cooling). Fig. 12 investigates the effect of rack IT load, with 'high IT load' corresponding to server power consumption as described in Section 2.3, and 'low IT load' denoting conditions wherein the total IT power consumption is halved by halving the number of servers. Here, the normalised power consumption at $\Delta p_{CH}$ = 5 Pa with high bypass is set at unity, with all other power consumptions shown as a proportion of this figure. $T_{amb}$ is set to 11 °C, and the results are shown with both server fan options. Very similar trends were observed with $T_{amb}$ = 30 °C.

## 4. Discussion

### 4.1. Accuracy and repeatability

Error bars are displayed in Fig. 10. The results of repeat tests were compared numerically with the original test results. This was achieved by carrying out a linear interpolation to estimate the air speed which would have been recorded in the original test at the pressure recorded for the relevant data point in the repeat test. Where the repeat reading was carried out at a lower pressure

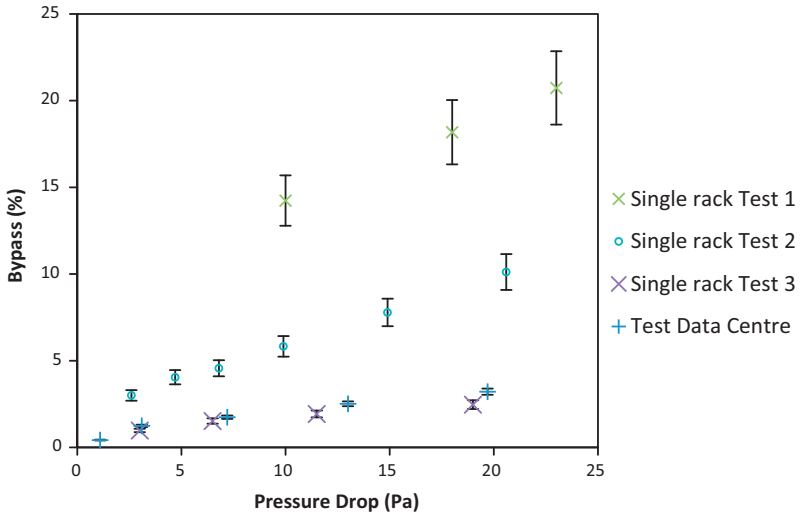


**Fig. 10.** Percentage bypass in the single rack and test DC experiments, with error bars indicated. KIMO HP15 manometer used for pressure readings in 'Single rack Test 1', Digitron 2080p used for all others.

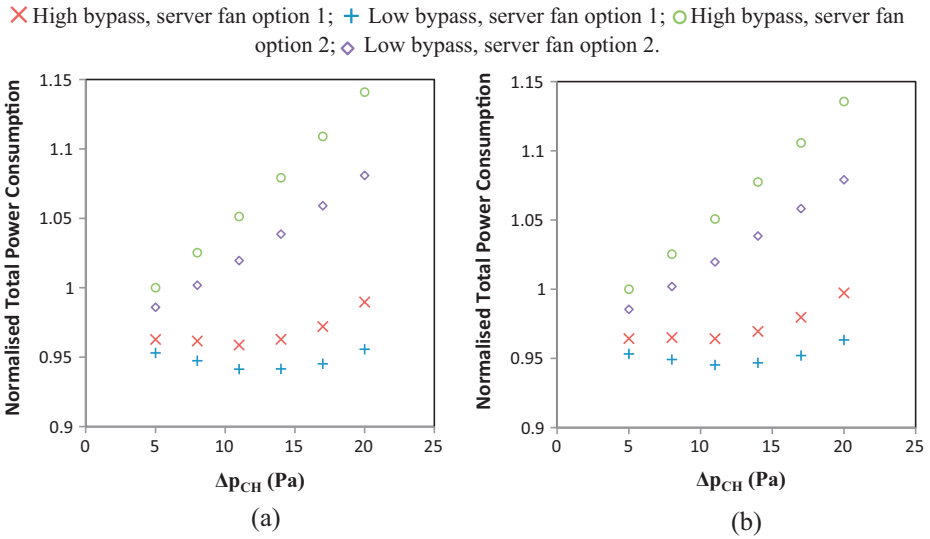


**Fig. 11.** Variation of total power consumption with cold aisle pressure, rack sealing and server fan speed option, with ambient temperature set to (a) 11 °C and (b) 30 °C.

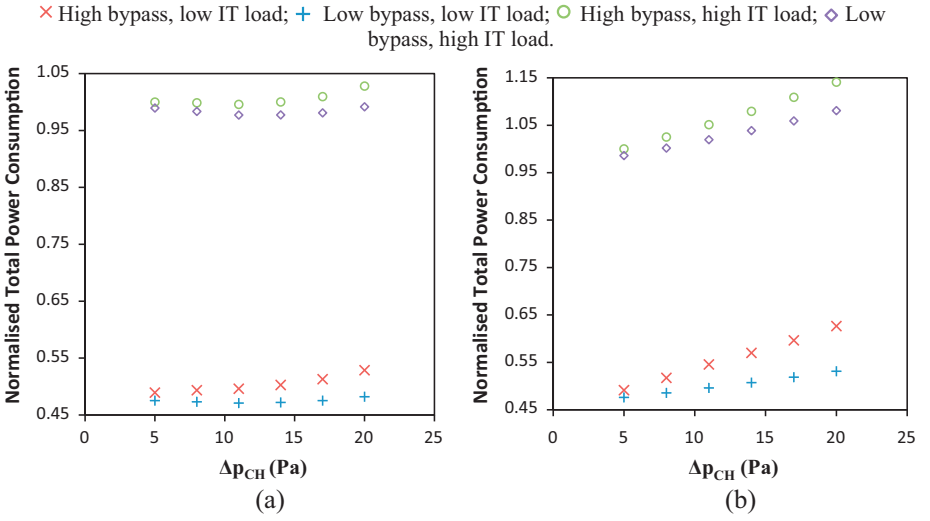


**Fig. 12.** Variation of total power consumption with cold aisle pressure, rack sealing and IT load, with ambient temperature set to 11 °C and server fans set to (a) Option 1 and (b) Option 2.

than any of the original readings, the interpolation was carried out between the next highest point and the origin. The percentage difference between the result of this interpolation and the air speed recorded at this pressure in the repeat test was recorded. The root mean square (RMS) percentage difference was 10.2% for the single rack tests, and 5.6% for the test DC. Hence, the error bars shown in Fig. 10 correspond to the range of percentage bypass corresponding to a variation in measured flow rate of ±10.2 and ±5.6% for the single rack and test DC results, respectively.

### 4.2. Observations on rack design

The results reported in Fig. 10 clearly show that significant quantities of air can bypass the servers by passing through the racks in a contained cold aisle system. A comparison of the results labelled 'Single rack Test 1' with those from the test DC shows that it is possible to significantly reduce rack bypass from the levels present in typical commercially available racks with no modifications. Comparing the results from Tests 1 and 2 shown in Fig. 10 demonstrates that simply applying 2 strips of foam to seal the most significant leakage paths can dramatically reduce rack bypass. The exact reduction in bypass varies from 54% to 62% over the range of 10–23 Pa. The authors propose that such measures could be easily retrofitted in a live DC, and could lead to a significant reduction in bypass. Some of the measures required to achieve the low levels of bypass shown for Test 3 via retrofitting were somewhat labour intensive, and would perhaps be unlikely to be replicated in a live DC. However, it was found to be possible to achieve similarly low levels of rack bypass using a re-designed rack, using parts available from the manufacturer, as can be seen from a comparison of the results of Test 3 with those for the test DC. This further indicates that bypass through the containment system was small, with rack bypass dominating.

### 4.3. Rack bypass levels and implications for energy efficiency

From Fig. 10 it can be seen that the untreated rack displays bypass levels of 14–19% at cold aisle pressures of 10-20 Pa. It is interesting to compare these figures with the bypass percentages reported in Section 2.1 for flow through a single empty slot in an otherwise populated rack (3.1–10.4% at $2<\Delta p_{CH}<20$), and the average of 50% bypass reported by Salim and Tozer for DCs not employ-

ing containment [20] (discussed in Section 1). The results suggest that bypass through racks is likely to be a significant component of overall bypass in DCs employing aisle containment, which should be considered after ensuring that blanking plates are in place wherever required. The measures undertaken to reduce bypass are shown to be very effective, with bypass reduced to 3.2% at 20 Pa in the test data centre. The level of pressurisation of the cold aisle has a significant impact on bypass.

Figs. 11 and 12 show that bypass through racks in contained aisles can significantly increase $E_T$. This is primarily due to an increase in $E_{ACU}$. The achievable reduction in $E_T$ depends strongly on $\Delta p_{CH}$, the response of server fans to $\Delta p_{CH}$, and the IT load density, ranging from 1% to 8.8%. It should be noted that the results also indicate the potential for control of $\Delta p_{CH}$ to minimise $E_T$. The results displayed in Fig. 11 show that the optimum $\Delta p_{CH}$ depends strongly on how server fan speeds respond to $\Delta p_{CH}$. This is because the increase in $E_{ACU}$ resulting from increasing $\Delta p_{CH}$ can be offset by the potential reduction in $E_{server\ fans}$. The results of Brady's experiments [61], discussed in Section 2.1, suggested that air driven through a server by aisle pressure may not cool the server effectively, hence server fans may still be required to maintain the desired CPU temperature. More experimental work is required to determine the exact effect of $\Delta p_{CH}$ on server fan speeds, but at present it may be assumed that the behaviour falls somewhere between Options 1 and 2 as implemented in the described model. The results displayed in Fig. 12 show that bypass and $\Delta p_{CH}$ have a stronger impact on $E_T$ when the DC is operating at a lower IT load. This is because the bypass percentage increases under these conditions due to falling server air flow rates, increasing the importance of $E_{ACU}$.

The effect of bypass and $\Delta p_{CH}$ on $E_{ACU}$ and $E_{server\ fans}$ dominates the impact of these factors on $E_T$. However, the COP of the cooling infrastructure, $COP_C$, is also affected by these factors. $COP_C$ is defined by Eq. (19). At $T_{amb}$ = 11 °C (i.e. with no mechanical cooling), and with server fan option 1 and maximum IT load, reducing $\Delta p_{CH}$ from 20 to 5 Pa reduces $COP_C$ by 7.4–8.0%, depending on the extent of bypass minimisation. Introducing best practice for bypass minimisation with $T_{amb}$ = 11 °C, server fan option 1 and maximum IT load reduces $COP_C$ by 1.5–2.2%, depending on the value of $\Delta p_{CH}$. These results show that increasing bypass leads to a slight increase in $COP_C$, which is caused by the increase in flow rate through the ACU and the resulting increase in $h$, as shown in Eq. (17). Setting $T_{amb}$ = 30 °C and using server fan option 2 both tend to reduce the changes in $COP_C$.

$$COP_C = \dot{Q}_{ACU}/(E_T - E_{servers} - E_{ACU}) \quad (19)$$

$T_{amb}$ (and the associated cooling method) has very little effect on the response of $E_T$ to the variables investigated. This is because, whilst $E_{CW}$ and $E_{chiller}$ increase slightly with bypass, changes in $E_{ACU}$ and $E_{server\ fans}$ dominate, and are unaffected by the ambient temperature.

Tests were also undertaken using the model to investigate the effect of the value of $n$ used in the heat exchanger modelling, with the finding that this had no significant impact on the results. Similarly, the model was modified so that the CW flow rate or temperature drop could be held constant, rather than being controlled to minimise $E_T$. Again, this was found not to have a significant impact on the results.

## 5. Conclusions

The experimental results and analysis presented have shown that significant levels of bypass can occur through server racks in DCs employing cold aisle containment. This is the first time that such bypass has been measured in the research literature, and the analysis presented is the first investigation into the impact of bypass on $E_T$. Up to 20% of cold air supplied to the cold aisle may bypass the servers, depending on the level of $\Delta p_{CH}$ and the extent to which leakage paths within server racks are blocked. A reduction in $E_T$ of 1–8.8% is predicted to be achievable via improved rack design or blocking of leakage paths, with the reduction being strongly influenced by $\Delta p_{CH}$, the IT power density and the response of server fan speed to cold aisle pressure. $E_T$ is also shown to be affected by $\Delta p_{CH}$, with an up to 16% reduction in $E_T$ being achievable through optimisation of $\Delta p_{CH}$, depending on the IT power density, response of server fan speed to cold aisle pressure and the extent to which rack leakage paths are blocked. The value of the optimum pressure differential between the hot and cold aisles, $\Delta p_{CH}$, also varies depending on these parameters. The system model developed is the first to investigate the effect of bypass and $\Delta p_{CH}$ on the total DC power consumption, $E_T$. Future work is needed to investigate the impact of the presence of servers on bypass levels. This will involve repeating the experiments in the test DC with the addition of servers.

## Acknowledgements

Morgan Tatchell-Evans would like to thank both Digiplex London 1 Ltd and The Engineering and Physical Sciences Research Council for funding this research (Grant EP/G036608/1).

Supporting data has been embargoed due to the commercially sensitive nature of the research and to allow for commercialisation of research findings. Further details about the nature of the data and conditions of access are available at http://dx.doi.org/10.5518/45.

## References

[1] International Energy Agency. World Energy Outlook 2014; 2014.
[2] Pérez-Lombard L, Ortiz J, Pout C. A review on buildings energy consumption information. Energy Build 2008;40:394–8. http://dx.doi.org/10.1016/j.enbuild.2007.03.007.
[3] Nejat P, Jomehzadeh F, Taheri MM, Gohari M, Majid MZA. A global review of energy consumption, $CO_2$ emissions and policy in the residential sector (with an overview of the top ten $CO_2$ emitting countries). Renew Sustain Energy Rev 2015;43:843–62. http://dx.doi.org/10.1016/j.rser.2014.11.066.
[4] Urge-Vorsatz D, Petrichenko K, Staniec M, Eom J. Energy use in buildings in a long-term perspective. Curr Opin Environ Sustain 2013;5:141–51. http://dx.doi.org/10.1016/j.cosust.2013.05.004.
[5] Chua KJ, Chou SK, Yang WM, Yan J. Achieving better energy-efficient air conditioning – a review of technologies and strategies. Appl Energy 2013;104:87–104. http://dx.doi.org/10.1016/j.apenergy.2012.10.037.
[6] Lin Z, Lee CK, Fong S, Chow TT, Yao T, Chan ALS. Comparison of annual energy performances with different ventilation methods for cooling. Energy Build 2011;43:130–6. http://dx.doi.org/10.1016/j.enbuild.2010.08.033.
[7] Xu H, Niu J. Numerical procedure for predicting annual energy consumption of the under-floor air distribution system. Energy Build 2006;38:641–7. http://dx.doi.org/10.1016/j.enbuild.2005.10.003.
[8] Oh MS, Ahn JH, Kim DW, Jang DS, Kim Y. Thermal comfort and energy saving in a vehicle compartment using a localized air-conditioning system. Appl Energy 2014;133:14–21. http://dx.doi.org/10.1016/j.apenergy.2014.07.089.
[9] Alajmi A, El-Amer W. Saving energy by using underfloor-air-distribution (UFAD) system in commercial buildings. Energy Convers Manag 2010;51:1637–42. http://dx.doi.org/10.1016/j.enconman.2009.12.040.
[10] Wagner J, Schäfer M, Phan L, Schlüter A, Rosano JH, Lin C-X. Localized climatisation of perishable products – solutions for increasing energy efficiency. In: Proc ASME 2014 int mech eng congr expo IMECE2014, Montreal, Canada; 2014.
[11] Schäfer M, Detzer R, Hesselbach J, Böhm S, Shinde P, Lin C-X. $CO_2$ and thermal gradient based demand-driven stratified ventilation—experimental and simulation study. HVAC&R Res 2013;19:676–92.
[12] Joshi Y, Kumar P. Introduction to data center energy flow and thermal management. In: Joshi Y, Kumar P, editors. Energy effic therm manag data centers. Springer Verlag; 2012.
[13] Beaty DL, Internal IT. Load profile variability. ASHRAE J 2013;55:72–4.
[14] Van Heddeghem W, Lambert S, Lannoo B, Colle D, Pickavet M, Demeester P. Trends in worldwide ICT electricity consumption from 2007 to 2012. Comput Commun 2014;50:64–76. http://dx.doi.org/10.1016/j.comcom.2014.02.008.
[15] Council of the Europeann Union. Presidency conclusions – Brussels, 29/30 October 2009; 2009. <http://www.consilium.europa.eu/uedocs/cms_data/docs/pressdata/en/ec/110889.pdf> [accessed November 16, 2015].

[16] The White House. U.S.–China joint announcement on climate change; 2014. <https://www.whitehouse.gov/the-press-office/2014/11/11/us-china-joint-announcement-climate-change> [accessed November 16, 2015].

[17] Newcombe L, Acton M, Booth J, Flucker S, Latham P, Strutt S, et al. Best practices for the EU code of conduct on data centres 2012; 2012. <http://re.jrc.ec.europa.eu/energyefficiency/pdf/CoC/Best Practices v3 0 8_2_ final release Dec 2011.pdf> [accessed September 12, 2013].

[18] U.S. Department of Energy and U.S. Environmental Protection Agency. Energy efficiency in data centers: recommendations for government-industry coordination; 2008. <http://www1.eere.energy.gov/manufacturing/tech_assistance/pdfs/data_center_wrkshp_report.pdf> [accessed January 13, 2014].

[19] Environment Agency. Umbrella climate change agreement for the standalone data centres; 2014. <https://www.gov.uk/government/uploads/system/uploads/attachment_data/file/336160/LIT_9990.pdf> [accessed September 15, 2014].

[20] Salim M, Tozer R. Data Centers' Energy Auditing and Benchmarking-Progress Update. ASHRAE winter conf, Orlando, FL; 2010. p. 109–17.

[21] European Commission. Code of conduct on data centre energy efficiency: endorser guidelines and registration form version 3.0.0; 2015. <http://iet.jrc.ec.europa.eu/energyefficiency/sites/energyefficiency/files/files/documents/ICT_CoC/endorser_guidelines_v3.0.0.pdf> [accessed May 18, 2015].

[22] Oró E, Depoorter V, Garcia A, Salom J. Energy efficiency and renewable energy integration in data centres. Strategies and modelling review. Renew Sustain Energy Rev 2015;42:429–45. http://dx.doi.org/10.1016/j.rser.2014.10.03.

[23] Shrivastava SK, Iyengar M, Sammakia BG, Schmidt R, Vangilder JW. Experimental-numerical comparison for a high-density data center: hot spot heat fluxes in excess of 500 W/ft 2, vol. 32; 2009. p. 166–72.

[24] Bhopte S, Iyengar M, Schmidt R, Sammakia B. Numerical and experimental study of the effect of underfloor blockages on data center performance. J Electron Packag 2011;133:11007.

[25] Cho J, Lim T, Kim BS. Measurements and predictions of the air distribution systems in high compute density (Internet) data centers. Energy Build 2009;41:1107–15. http://dx.doi.org/10.1016/j.enbuild.2009.05.017.

[26] Cho J, Kim BS. Evaluation of air management system's thermal performance for superior cooling efficiency in high-density data centers. Energy Build 2011;43:2145–55. http://dx.doi.org/10.1016/j.enbuild.2011.04.025.

[27] Tsuchiya T, Suwa Y, Ooka R. Experimental study of airflow designs for data centers. J Asian Archit Build Eng 2014;13:491–8.

[28] Srinarayana N, Fakhim B, Behnia M, Armfield SW. Thermal performance of an air-cooled data center with raised-floor and non-raised-floor configurations. Heat Transf Eng 2014;35:384–97. http://dx.doi.org/10.1080/01457632.2013.828559.

[29] Patankar SV. Airflow and cooling in a data center. J Heat Transfer 2010;132:73001.

[30] Alkharabsheh SA, Sammakia BG, Shrivastava SK. Experimentally validated computational fluid dynamics model for a data center with cold aisle containment. J Electron Packag 2015:137. http://dx.doi.org/10.1115/1.402934.

[31] Schmidt R, Vallury A, Iyengar M. Energy savings through hot and cold aisle containment configurations for air cooled servers in data centers. ASME 2011 pacific rim tech conf exhib packag integr electron photonic syst, Portland, Oregon; 2011. p. 611–6.

[32] Shrivastava SK, Calder AR, Ibrahim M. Quantitative comparison of air containment systems. Therm thermomechanical phenom electron syst (ITherm), 2012 13th IEEE intersoc conf, San Diego, CA; 2012. p. 68–77.

[33] Pelley S, Meisner D, Wenisch TF, VanGilder JW. Understanding and abstracting total data center power. Work energy-efficient des, Austin, TX; 2009.

[34] Arghode VK, Sundaralingam V, Joshi Y, Phelps W. Thermal characteristics of open and contained data center cold aisle. J Heat Transf – Trans ASME 2013:135.

[35] Choo K, Galante RM, Ohadi MM. Energy consumption analysis of a medium-size primary data center in an academic campus. Energy Build 2014;76:414–21. http://dx.doi.org/10.1016/j.enbuild.2014.02.042.

[36] Demetriou DW, Khalifa HE. Optimization of enclosed aisle data centers using bypass recirculation. J Electron Packag 2012:134.

[37] Joshi Y, Kumar P. Fundamentals of data center airflow management. In: Joshi Y, Kumar P, editors. Energy effic therm manag data centers. New York: Springer; 2012.

[38] Breen TJ, Walsh EJ, Punch J, Shah AJ, Bash CE. From chip to cooling tower data center modeling: influence of server inlet temperature and temperature rise across cabinet. J Electron Packag 2012:133. http://dx.doi.org/10.1115/1.400327.

[39] ASHRAE T.C. 9.9. Thermal guidelines for data processing environments – expanded data center classes and usage guidance. Atlanta; 2011.

[40] Uptime Institute. Data Center Industry Survey; 2013.

[41] Alkharabsheh SA, Muralidharan B, Ibrahim M, Shrivastava SK, Sammakia BG. Open and contained cold aisle experimentally validated CFD model implementing CRAC and server fan curves for a data center test laboratory. ASME 2013 int tech conf exhib packag integr electron photonic microsystems, Burlingame; 2013.

[42] Emerson Network Power. Optimized energy efficiency with controlled cold aisle containments; 2014. <http://www.emersonnetworkpower.com/en-EMEA/Latest-Thinking/white-papers/Documents/Optimized-energy-efficiency-with-controlled-cold-aisle-containments.pdf> [accessed August 14, 2014].

[43] Honeybill A. Air segregation: how to measure effectiveness; 2015. <http://www.upsite.com/blog/air-segregation-how-to-measure-effectiveness/> [accessed September 04, 2015].

[44] Kennedy D. Server leakage and cooling. Datacenter Dyn Focus 2013;3:50–2.

[45] Airedale. LogiCool InRak 2012:21. <http://airedalecoolingsolutions.co.uk/updates/downloads/TM_INRAK_UK.pdf> [accessed September 04, 2015].

[46] Sundaralingam V, Arghode VK, Joshi Y, Phelps W. Experimental characterization of various cold aisle containment configurations for data centers. J Electron Packag 2015:137. http://dx.doi.org/10.1115/1.402852.

[47] Arghode VK, Joshi Y. Room level modeling of air flow in a contained data center aisle. J Electron Packag 2014;136:11011.

[48] Nguyen A-T, Reiter S, Rigo P. A review on simulation-based optimization methods applied to building performance analysis. Appl Energy 2014;113:1043–58. http://dx.doi.org/10.1016/j.apenergy.2013.08.061.

[49] Breen TJ, Walsh EJ, Punch J, Shah AJ, Bash CE, Rubenstein B, et al. From chip to cooling tower data center modeling: influence of air-stream containment on operating efficiency. J Electron Packag 2012:134.

[50] Wemhoff AP, del Valle M, Abbasi K, Ortega A. Thermodynamic modeling of data center cooling systems. In: Proc ASME 2013 int tech conf exhib packag integr electron. Photonic Microsystems, Burlingame, CA; 2013.

[51] Patel CD, Sharma RK, Bash CE, Beitelmal M. Energy flow in the information technology stack: coefficient of performance of the ensemble and its impact on the total cost of ownership; 2006. <http://www.hpl.hp.com/techreports/2006/HPL-2006-55.pdf> [accessed August 11, 2015].

[52] Heydari A. Thermodynamics energy efficiency analysis and thermal modeling of data center cooling using open and closed-loop cooling systems, Vancouver; 2007.

[53] Iyengar M, Schmidt R. Analytical modeling for thermodynamic characterization of data center cooling systems. J Electron Packag 2009;131:21009.

[54] Microsystems S. SunFire V20z Server; 2003. <http://www.grycap.upv.es/img/repos/Sun Fire V20z.pdf> [accessed August 07, 2015].

[55] Granger RA. Laminar pipe flow. Fluid mech. New York, NY, USA: Dover Publications; 1995.

[56] Shaughnessy EJ. Flow in pipes and ducts. Introd to fluid mech. Oxford, UK: Oxford University Press; 2005.

[57] Jones Jr OC. An improvement in the calculation of turbulent friction in rectangular ducts. J Fluids Eng 1976;98:173–80.

[58] Poling BE, Thomson GH, Friend DG, Rowley RL, Wilding WV. Physical and chemical data. In: Green DW, Perry RH, editors. Perry's chem Eng Handbook2. London: McGraw-Hill; 2008.

[59] Miller R. Emerson: 10 Common Data Center Surprises; 2012. <http://www.datacenterknowledge.com/archives/2012/03/21/emerson-10-common-data-center-surprises/> [accessed August 13, 2014].

[60] Demetriou DW, Khalifa HE. Energy modeling of air-cooled data centers: Part II—The effect of recirculation on the energy optimization of open-aisle, air-cooled data centers. ASME 2011 pacific rim tech conf exhib packag integr electron photonic syst, Portland; 2011.

[61] Brady GA. An interdisciplinary investigation into energy use and efficiency within the data centre. Ph.D. thesis. University of Leeds; 2014 [unpublished].

[62] Kennedy D. Ramification of server airflow leakage in data centers with aisle containment; 2012. <http://tateinc.com/pdf/ramification_leakage_aisle_containment.pdf> [accessed August 14, 2014].

[63] Patterson MK. The effect of data center temperature on energy efficiency; 2008. <http://ieeexplore.ieee.org/stamp/stamp.jsp?arnumber=04544393> [accessed March 11, 2014].

[64] Talaber R, Brey T, Lamers L. Using virtualization to improve data center efficiency; 2009. <http://www.thegreengrid.org/~/media/WhitePapers/White Paper 19 – Using Virtualization to Improve Data Center Efficiency.pdf?lang=en> [accessed August 05, 2014].

[65] Tighe M, Keller G, Bauer M, Lutfiyya H. DCSim: a data centre simulation tool for evaluating dynamic virtualized resource management. In: 8th Int conf netw serv manag, Las Vegas; 2012.

[66] Wilkie T. High-Performance Computing – Cool ways to save energy; 2015. <http://www.scientific-computing.com/features/feature.php?feature_id=460> [accessed February 17, 2016].

[67] Venkatraman A. Enterprises, scientists and academics turn to public cloud for HPC; 2014. <http://www.computerweekly.com/feature/Enterprises-scientists-and-academics-turn-to-public-cloud-for-HPC> [accessed February 17, 2016].

[68] Barroso LA, Holzle U. The case for energy-proportional computing. Computer (Long Beach Calif) 2007;40:33.

[69] Heller B, Seetharaman S, Mahadevan P, Yiakoumis Y, Sharma P, Banerjee S, et al. ElasticTree: saving energy in data center networks. In: NSDI'10 proc 7th USENIX conf networked syst des implement, Berkeley, CA; 2010. p. 17.

[70] Shirayanagi H, Yamada H, Kono K. Honeyguide: a VM migration-aware network topology for saving energy consumption in data center networks. 2012 IEEE symp comput commun, 345 E 47th st, New York, NY 10017 USA: IEEE; 2012. p. 460–7.

[71] Newcombe L. Data centre energy efficiency metrics; 2010. <http://bcs.org/upload/pdf/data-centre-energy.pdf> [accessed September 04, 2015].

[72] Omega Engineering Limited. HHF2005HW; 2014. <http://www.omega.co.uk/pptst/HHF2005HW.html> [accessed August 23, 2014].

[73] TSI. Anemometer TA2 Range; 2014. <http://www.tsi.com/airflow-instruments-thermal-anemometer-ta2-range/> [accessed August 12, 2014].

[74] Digitron. 2000 Series Technical Data Sheet, n.d. <http://docs-europe.electrocomponents.com/webdocs/0785/0900766b8078507e.pdf> [accessed August 23, 2014].
[75] KIMO Instruments. HP series inclined liquid column manometers; 2010. <http://kimouk.com/datasheets-manuals/manometers/Manometers/FT-HP.pdf> [accessed August 11, 2014].
[76] The Met Office. Mean temperature – annual average: 1971–2000, n.d. <http://www.metoffice.gov.uk/public/weather/climate/gcpuckhb6#?region=southernengland> [accessed August 24, 2015].
[77] The Green Grid. Updated air-side free cooling maps: the impact of ASHRAE 2011 allowable ranges; 2012. <http://www.thegreengrid.org/~/media/WhitePapers/WP46UpdatedAirsideFree CoolingMapsTheImpactofASHRAE2011AllowableRanges.pdf?lang=en> [accessed March 27, 2014].
[78] Schneider Electric. Uniflair LE chilled water air conditioners, n.d. http://www.schneider-electric.com/ww/en/download/document/APC_KKRZ-8LAPNS_R6_EN_SRC [accessed September 07, 2015].
[79] Incropera FP, Dewitt DP. Heat exchangers. Fundam heat mass transf. 5th ed. New York: John Wiley & Sons, Ltd.; 2002.
[80] Wang C-C, Chang Y-J. Sensible heat and friction characteristics of plate fin-and-tube heat exchangers having plane fins. Int J Refrig 1996;19:223–30.
[81] Rabas T, Eckels P, Sabatino R. The effect of fin density on the heat-transfer and pressure-drop performance of low-finned tube banks. Chem Eng Commun 1981;10:127–47.
[82] Winterton RHS. Where did the Dittus and Boelter equation come from? Int J Heat Mass Transf 1998;41:809–10.
[83] Airedale. DeltaChill Air Cooled; 2014. <http://www.airedale.com/web/Products/Chillers/DeltaChill-DeltaChill-FreeCool-110kW-1080kW.htm> [accessed September 08, 2015].